

Graphene: new bridge between condensed matter physics and quantum electrodynamics

M. I. Katsnelson¹ and K. S. Novoselov²

¹*Institute for Molecules and Materials,*

Radboud University Nijmegen, 6525 ED Nijmegen, The Netherlands

²*Manchester Centre for Mesoscience and Nanotechnology,*

University of Manchester, Manchester M13 9PL, UK

Abstract

Graphene is the first example of truly two-dimensional crystals - it's just one layer of carbon atoms. It turns out to be a gapless semiconductor with unique electronic properties resulting from the fact that charge carriers in graphene demonstrate charge-conjugation symmetry between electrons and holes and possess an internal degree of freedom similar to "chirality" for ultrarelativistic elementary particles. It provides unexpected bridge between condensed matter physics and quantum electrodynamics (QED). In particular, the relativistic Zitterbewegung leads to the minimum conductivity of order of conductance quantum e^2/h in the limit of zero doping; the concept of Klein paradox (tunneling of relativistic particles) provides an essential insight into electron propagation through potential barriers; vacuum polarization around charge impurities is essential for understanding of high electron mobility in graphene; index theorem explains anomalous quantum Hall effect.

Keywords: Graphene; Transport Properties; Electron Mobility; Scattering Processes; Quantum Hall Effect; Index Theorem; Minimal Conductivity; Tunneling; Klein Paradox; Zitterbewegung.

Introduction

The variety of crystallographic forms of carbon places this element into the focus of attention both in terms of basic research as well as applications. The *three-dimensional* crystallographic forms - graphite and diamond - are known from the ancient times, and are widely used in industrial applications. Recently discovered *zero-dimensional* (fullerenes or cage molecules^{1,2,3}) and *one-dimensional* (carbon nanotubes⁴) forms are now extensively studied due to its' remarkable and, often, unique mechanical and electronic properties. At the same time, despite very intensive research in the area, no any *two-dimensional* form of carbon has been known until very recently.

Ironically, this elusive two-dimensional form (dubbed graphene), is, probably, the best theoretically studied carbon allotrope. Graphene - planar, hexagonal arrangements of carbon atoms has been the starting point in all calculations on graphite, carbon nanotubes and fullerenes since late 40s⁵. However, its' experimental discovery has been postponed till 2004 when a technique called micromechanical cleavage has been employed to obtain first graphene crystals^{6,7}. The observation of a peculiar spectrum of charge carriers and anomalous quantum Hall effect (QHE) in graphene^{8,9} has initiated enormously growing interest to this field (for review, see Refs.^{10,11}).

One of the most interesting aspects of the physics of graphene is that it provides a novel example of a “feedback” of condensed matter and material science on the fundamental physics. Of course, this is not an unique case; archetypical examples are the concept of spontaneously broken symmetry playing a crucial role in modern high energy physics and quantum field theory¹² and the use of Mössbauer effect to check the general relativity theory¹³. At the same time, such relations are rather rare and always turn out to be very fruitful. Actually, discovery of graphene has opened new ways to study some basic quantum relativistic phenomena which have always been considered as very exotic. Probably the most clear example is the Klein paradox^{14,15}, that is, a property of relativistic quantum particles to penetrate with a probability of the order of unity through very high and broad potential barriers. Previously it was discussed only for experimentally unattainable (or very hard to reach) situations such as particle-antiparticle pair creation at the black hole evaporation, or vacuum breakdown at collisions of super-heavy nuclei. At the same time, it appeared to be relevant for graphene-based electronics¹⁶. Here we discuss similarities and differences

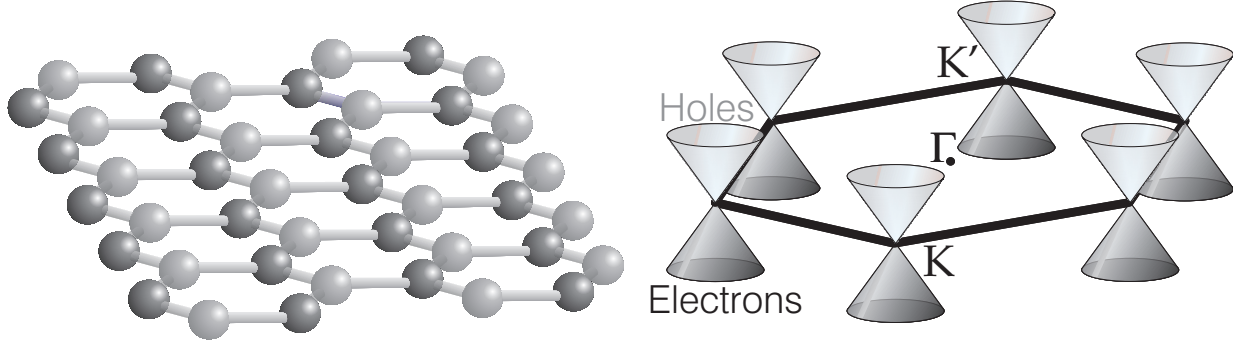


FIG. 1: Left: Crystallographic structure of graphene. Atoms from different sublattices (A and B) are marked by different shades of gray. Right: Band structure of graphene in the vicinity of the Fermi level. Conductance band touches valence band at K and K' points.

between physics of charge carriers in graphene and quantum electrodynamics (QED).

I. ELECTRONIC STRUCTURE OF GRAPHENE

From the point of view of its electronic properties, graphene is a two-dimensional zero-gap semiconductor with the energy spectrum shown schematically in Fig. 1 and its low-energy quasiparticles formally described by the Dirac-like Hamiltonian^{17,18,19}

$$\hat{H}_0 = -i\hbar v_F \sigma \nabla \quad (1)$$

where $v_F \approx 10^6$ ms⁻¹ is the Fermi velocity, and $\sigma = (\sigma_x, \sigma_y)$ are the Pauli matrices. Neglecting many-body effects, this description is accurate theoretically^{17,18,19} and has also been proven experimentally^{8,9} by measuring the energy-dependent cyclotron mass in graphene (which yields its linear energy spectrum) and, most clearly, by the observation of a relativistic analogue of the integer QHE which will be discussed below.

The fact that charge carriers in graphene are described by the Dirac-like equation (1) rather than the usual Schrödinger equation can be seen as a consequence of graphene's crystal structure, which consists of two equivalent carbon sublattices A and B^{17,18,19} (see Fig. 1). Quantum mechanical hopping between the sublattices leads to the formation of two energy bands, and their intersection near the edges of the Brillouin zone yields the conical energy spectrum near the “Dirac” points K and K' . As a result, quasiparticles in graphene

exhibit the linear dispersion relation $E = \hbar k v_F$, as if they were massless relativistic particles, with the role of the speed of light played by the Fermi velocity $v_F \approx c/300$. Due to the linear spectrum, one can expect that graphene's quasiparticles behave differently from those in conventional metals and semiconductors where the energy spectrum can be approximated by a parabolic (free-electron-like) dispersion relation.

Although the linear spectrum is important, it is not the only essential feature that underpins the description of quantum transport in graphene by the Dirac equation. Above zero energy, the current carrying states in graphene are, as usual, electron-like and negatively charged. At negative energies, if the valence band is not completely filled, its unoccupied electronic states behave as positively charged quasiparticles (holes), which are often viewed as a condensed-matter equivalent of positrons. Note however that electrons and holes in condensed matter physics are normally described by separate Schrödinger equations, which are not in any way connected (as a consequence of the Seitz sum rule²⁰, the equations should also involve different effective masses). In contrast, electron and hole states in graphene are interconnected, exhibiting properties analogous to the charge-conjugation symmetry in QED^{18,19}. For the case of graphene, the latter symmetry is a consequence of its crystal symmetry because graphene's quasiparticles have to be described by two-component wavefunctions, which is needed to define relative contributions of sublattices A and B in the quasiparticles' make-up. The two-component description for graphene is very similar to the one by spinor wavefunctions in QED but the "spin" index for graphene indicates sublattices rather than the real spin of electrons and is usually referred to as pseudospin σ .

There are further analogies with QED. The conical spectrum of graphene is the result of intersection of the energy bands originating from sublattices A and B (see Fig. 1) and, accordingly, an electron with energy E propagating in the positive direction originates from the same branch of the electronic spectrum as the hole with energy $-E$ propagating in the opposite direction. This yields that electrons and holes belonging to the same branch have pseudospin σ pointing in the same direction, which is parallel to the momentum for electrons and antiparallel for holes. This allows one to introduce chirality¹⁹, that is formally a projection of pseudospin on the direction of motion, which is positive and negative for electrons and holes, respectively. The term "chirality" is often used to refer to the additional built-in symmetry between electron and hole parts of graphene's spectrum and is analogous (although not completely identical^{18,21}) to the chirality in three-dimensional QED.

An alternative view on the origin of the chirality in graphene is based on the concept of “Berry phase”²². Since the electron wave function is a two-component spinor, it has to change sign when the electron moves along the close contour. Thus the wave function gains an additional phase $\phi = \pi$.

The analogy with the field theory takes a very interesting twist, should we take into account that a sheet of graphene must always be corrugated. The fact that graphene crystals always exhibit some finite local curvature can be considered as a consequence of the Mermin-Wagner theorem, and has been confirmed experimentally both for graphene samples resting on a substrate²³, as well as for free-hanging graphene films²⁴.

It is well known that harmonic approximation in the two-dimensional case doesn’t produce a solution with long-range order^{25,26,27,28}. One can see this as bending instabilities, due to soft long-wavelength phonons, lead to membrane crumpling²⁹. Anharmonic coupling between bending and stretching modes changes the situation drastically and prevents the crumpling^{29,30,31}. However, the membrane should be rippled in a sense that typical fluctuations in the direction perpendicular to the surface $h(x, y)$ has a scale of order of $a(L/a)^\zeta \gg a$ where a is the lattice constant, L is the size of the sample and ζ is the roughness exponent. The latter can be estimated as $\zeta \simeq 0.6$ ^{29,31}. For a typical sample size $L \sim 1\mu\text{m}$, the typical amplitude of the corrugation for free-hanging membrane at room temperature was estimated as 0.5 nm, with their characteristic size being about 5 nm²⁴.

These ripples lead to important consequences for the electronic structure of graphene. The nearest-neighbor hopping integral γ turns out to be fluctuating due to its dependence on the deformation tensor²⁹

$$\bar{u}_{ij} = \frac{1}{2} \left(\frac{\partial u_i}{\partial x_j} + \frac{\partial u_j}{\partial x_i} + \frac{\partial u_k}{\partial x_i} \frac{\partial u_k}{\partial x_j} + \frac{\partial h}{\partial x_i} \frac{\partial h}{\partial x_j} \right) \quad (2)$$

where $x_i = (x, y)$ are coordinates in the plane and u_i are corresponding components of the displacement vector:

$$\gamma = \gamma_0 + \left(\frac{\partial \gamma}{\partial \bar{u}_{ij}} \right)_0 \bar{u}_{ij}. \quad (3)$$

Taking into account this inhomogeneity in a standard tight-binding description of the electronic structure of graphene⁵ one can obtain. instead of Eq.(1) an effective Dirac-like Hamiltonian describing electron states near the K -point:

$$H = v_F \sigma \left(-i\hbar \nabla - \frac{e}{c} \mathcal{A} \right) \quad (4)$$

where $v_F = \sqrt{3}\gamma_0 a/2\hbar$ and \mathcal{A} is the “vector potential” connected with the deviations of the hopping parameters γ_i from their unperturbed value γ_0 :

$$\begin{aligned}\mathcal{A}_x &= \frac{c}{2ev_F} (\gamma_2 + \gamma_3 - 2\gamma_1), \\ \mathcal{A}_y &= \frac{\sqrt{3}c}{2ev_F} (\gamma_3 - \gamma_2),\end{aligned}\quad (5)$$

where the nearest neighbors with vectors $(-a/\sqrt{3}, 0); (a/2\sqrt{3}, -a/2); (a/2\sqrt{3}, a/2)$ are labelled 1,2, and 3, correspondingly. This means that the roughness fluctuations acts on the electronic structure near the K -point as an Abelian gauge field³² which is equivalent to the action of random magnetic field. This means that the bending of graphene violates the time-reversal symmetry for a given valley; of course, the Umklapp processes between K and K' points will restore this symmetry. As was suggested in Ref.²³ these effective magnetic fields are responsible for suppression of the weak localization effects in graphene.

Whereas smooth deformation of the graphene sheets produces gauge field similar to electromagnetic one, different topological defects in graphene inducing inter-valley (Umklapp) processes can be considered as sources of a non-Abelian gauge field; corresponding analogy with gravitation was discussed in Refs.^{33,34}.

In relativistic quantum mechanics, chirality is a consequence of particle-antiparticle symmetry, which also guarantees linear energy spectrum for massless particles. The discovery of graphene opens a unique opportunity, to investigate *chiral* particles with *parabolic (non-relativistic)* energy spectrum. Quasiparticle with such unusual properties can be found in *bilayer* graphene³⁵. For two graphene layers, the nearest-neighbor tight-binding approximation predicts a gapless state with *parabolic* touching in K and K' points^{35,36} (instead of conical band crossing in graphene). The electronic spectrum in this approximation is described by a single-particle Hamiltonian^{35,36}

$$H = \begin{pmatrix} 0 & -(p_x - ip_y)^2 / 2m \\ -(p_x + ip_y)^2 / 2m & 0 \end{pmatrix} \quad (6)$$

where $p_i = -i\hbar\partial/\partial x_i$ are electron momenta operators and m is the effective mass. Here we neglected higher-order hopping processes which are important only for very low Fermi energies. More accurate consideration³⁷ gives a very small band overlap (about 1.6 meV) but at larger energies bilayer graphene can be treated as a gapless semiconductor. At the

same time, electronic states are still characterized by chirality and by non-trivial Berry phase $2\pi^{35,36}$ (in contrast to the case of graphene, where the Berry phase was found to be $\pi^{8,9}$).

II. CHIRAL TUNNELING AND THE KLEIN PARADOX

The term Klein paradox^{14,15,16} usually refers to a counterintuitive relativistic process in which an incoming electron starts penetrating through a potential barrier if its height V_0 exceeds twice the electron's rest energy mc^2 (where m is the electron mass and c the speed of light). In this case, the transmission probability T depends only weakly on the barrier height, approaching the perfect transparency for very high barriers, in stark contrast to the conventional, nonrelativistic tunneling where T exponentially decays with increasing V_0 . This relativistic effect can be attributed to the fact that a sufficiently strong potential, being repulsive for electrons, is attractive for positrons and results in positron states inside the barrier, which align in energy with the electron continuum outside. Matching between electron and positron wavefunctions across the barrier leads to the high-probability tunneling described by the Klein paradox.

One can think about non-relativistic quantum mechanical tunneling through a potential barrier in terms of indeterminacy principle. Since momentum and coordinates of a particle can not be measured simultaneously a particle can propagate through a classically forbidden region where the momentum is formally imaginary, and only coordinates are well defined. In *relativistic* quantum mechanics even coordinate itself cannot be measured with arbitrary accuracy, due to pair creation at this measurement. In other words, the Klein paradox illustrates that the relativistic quantum mechanics can be consistently formulated only in terms of fields rather than individual particles³⁸.

Although Klein's gedanken experiment is now well understood, the notion of paradox is still used widely, perhaps because the effect has never been observed experimentally. Indeed, its observation requires a potential drop $\approx mc^2$ over the Compton length \hbar/mc , which yields enormous electric fields^{39,40} ($\mathcal{E} > 10^{16}V/cm$) and makes the effect relevant only for such exotic situations as, for example, positron production around super-heavy nuclei^{39,40} with charge $Z \geq 170$ or evaporation of black holes through generation of particle-antiparticle pairs near the event horizon⁴¹. At the same time, electronic structure of graphene provides us an unique opportunity for easy experimental realization of the Klein ultrarelativistic tunneling

in $p - n$ junctions^{16,42,43}.

Let us consider for simplicity the potential barrier that has a rectangular shape and is infinite along the y -axis:

$$V(x) = \begin{cases} V_0, & 0 < x < D, \\ 0 & \text{otherwise.} \end{cases} \quad (7)$$

This local potential barrier inverts charge carriers underneath it, creating holes playing the role of positrons. For simplicity, we assume in Eq.(7) infinitely sharp edges, which allows a direct link to the case usually considered in QED^{14,15}. The sharp-edge assumption is justified if the Fermi wavelength λ of quasiparticles is much larger than the characteristic width of the edge smearing, which in turn should be larger than the lattice constant (to disallow Umklapp scattering between different valleys in graphene). Such a barrier can be created by the electric field effect using a thin insulator or by local chemical doping^{7,8,9}. Importantly, Dirac fermions in graphene are massless and, therefore, there is no formal theoretical requirement for the minimal electric field \mathcal{E} to form positron-like states under the barrier. To create a well-defined barrier in realistic graphene samples with a disorder, fields $\mathcal{E} \approx 10^5 V/cm$ routinely used in experiments^{7,9} should be sufficient, which is eleven orders of magnitude lower than the fields necessary for the observation of the Klein paradox for elementary particles.

It is straightforward to solve the tunneling problem for Dirac electrons¹⁶. We assume that the incident electron wave propagates at an angle ϕ with respect to the x axis and then try the components of the Dirac spinor ψ_1 and ψ_2 for the Hamiltonian $H = H_0 + V(x)$ in the following form:

$$\begin{aligned} \psi_1(x, y) &= \begin{cases} (e^{ik_x x} + r e^{-ik_x x}) e^{ik_y y}, & x < 0, \\ (a e^{iq_x x} + b e^{-iq_x x}) e^{ik_y y}, & 0 < x < D, \\ t e^{ik_x x + ik_y y}, & x > D, \end{cases} \\ \psi_2(x, y) &= \begin{cases} s (e^{ik_x x + i\phi} - r e^{-ik_x x - i\phi}) e^{ik_y y}, & x < 0, \\ s' (a e^{iq_x x + i\theta} - b e^{-iq_x x - i\theta}) e^{ik_y y}, & 0 < x < D, \\ s t e^{ik_x x + ik_y y + i\phi}, & x > D, \end{cases} \end{aligned} \quad (8)$$

where $k_F = 2\pi/\lambda$ is the Fermi wavevector, $k_x = k_F \cos \phi$ and $k_y = k_F \sin \phi$ are the wavevector components outside the barrier, $q_x = \sqrt{(E - V_0)^2 / \hbar^2 v_F^2 - k_y^2}$, $\theta = \tan^{-1}(k_y/q_x)$ is the refraction angle, $s = \text{sign}E$, $s' = \text{sign}(E - V_0)$. Requiring the continuity of the wave-

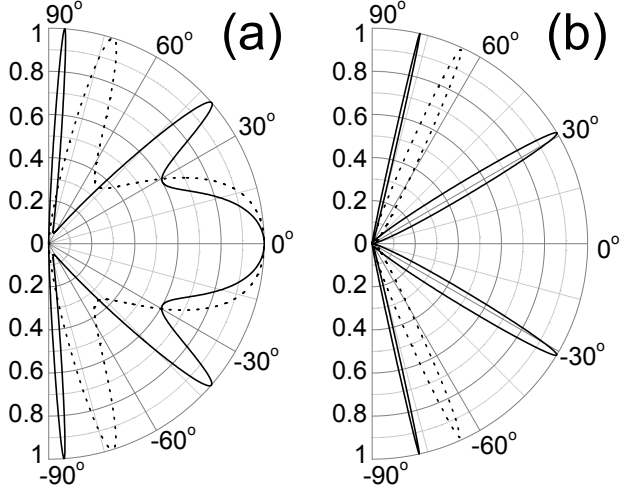


FIG. 2: Transmission probability T through a 100-nm-wide barrier as a function of the incident angle for single- (a) and bi-layer (b) graphene. The electron concentration n outside the barrier is chosen as $0.5 \times 10^{12} \text{ cm}^{-2}$ for all cases. Inside the barrier, hole concentrations p are 1×10^{12} and $3 \times 10^{12} \text{ cm}^{-2}$ for solid and dashed curves, respectively (such concentrations are most typical in experiments with graphene). This corresponds to the Fermi energy E of incident electrons ≈ 80 and 17 meV for single- and bi-layer graphene, respectively, and $\lambda \approx 50 \text{ nm}$. The barrier heights are (a) 200 and (b) 50 meV (solid curves) and (a) 285 and (b) 100 meV (dashed curves).

function by matching up coefficients a, b, t, r , we can find the the reflection coefficient r .

Fig. 2a shows examples of the angular dependence of transmission probability $T = |t|^2 = 1 - |r|^2$ calculated using the above expression. The barrier remains *always* perfectly transparent for angles close to the normal incidence $\phi = 0$. The latter is the feature unique to massless Dirac fermions and directly related to the Klein paradox in QED. One can understand this perfect tunneling in terms of the conservation of pseudospin. Indeed, in the absence of pseudospin-flip processes (such processes are rare as they require a short-range potential, which would act differently on A and B sites of the graphene lattice), an electron moving to the right can be scattered only to a right-moving electron state or left-moving hole state. The matching between directions of pseudospin σ for quasiparticles inside and outside the barrier results in perfect tunneling. In the strictly one-dimensional case, such perfect transmission of Dirac fermions has been discussed in the context of electron trans-

port in carbon nanotubes^{44,45}. This is also the case for the two-dimensional (2D) problem of graphene which can be directly proven by consideration of the Lippmann-Schwinger equation for scattering of arbitrary scalar potential (see Ref.¹⁶, supplementary information).

To elucidate which features of the anomalous tunneling in graphene are related to the linear dispersion and which to the pseudospin and chirality of the Dirac spectrum, it is instructive to consider the same problem for bilayer graphene¹⁶. Although “massive chiral fermions” with parabolic spectrum near the touching point and Berry phase 2π do not exist in the field theory their existence in the condensed matter physics (confirmed experimentally³⁵) offers a unique opportunity to clarify the importance of chirality in the relativistic tunneling problem described by the Klein paradox.

Charge carriers in bilayer graphene are described by an off-diagonal Hamiltonian (6) which yields a gapless semiconductor with chiral electrons and holes having a finite mass m . An important formal difference between the tunneling problems for single- and bilayer graphene is that in the latter case there are *four* possible solutions for a given energy $E = \pm \hbar^2 k_F^2 / 2m$. Two of them correspond to propagating waves and the other two to evanescent ones. Accordingly, for constant potential V_i , eigenstates of Hamiltonian (6) should be written as

$$\begin{aligned}\psi_1(x, y) &= (a_i e^{ik_{ix}x} + b_i e^{-ik_{ix}x} + c_i e^{\kappa_{ix}x} + d_i e^{-\kappa_{ix}x}) e^{ik_y y} \\ \psi_2(x, y) &= s_i \left(a_i e^{ik_{ix}x+2i\phi_i} + b_i e^{-ik_{ix}x-2i\phi_i} - c_i h_i e^{\kappa_{ix}x} - \frac{d_i}{h_i} e^{-\kappa_{ix}x} \right) e^{ik_y y}\end{aligned}\quad (9)$$

where

$$\begin{aligned}s_i &= \text{sign}(V_i - E); \quad \hbar k_{ix} = \sqrt{2m|E - V_i|} \cos \phi_i; \quad \hbar k_{iy} = \sqrt{2m|E - V_i|} \sin \phi_i \\ \kappa_{ix} &= \sqrt{k_{ix}^2 + 2k_{iy}^2}; \quad h_i = \left(\sqrt{1 + \sin^2 \phi_i} - \sin \phi_i \right)^2.\end{aligned}$$

To find the transmission coefficient through barrier (7), one should set $d_1 = 0$ for $x < 0$, $b_3 = c_3 = 0$ for $x > D$ and satisfy the continuity conditions for both components of the wavefunction and their derivatives. For the case of an electron beam that is incident normally ($\phi = 0$) and low barriers $V_0 < E$ (over-barrier transmission), we obtain $\psi_1 = -\psi_2$ both outside and inside the barrier, and the chirality of fermions in bilayer graphene does not manifest itself. In this case, scattering at the barrier (7) is the same as for electrons described by the Schrödinger equation. However, for any finite ϕ (even in the case $V_0 < E$), waves localized at the barrier interfaces are essential to satisfy the boundary conditions.

The most intriguing behavior is found for $V_0 > E$, where electrons outside the barrier transform into holes inside it, or vice versa. Examples of the angular dependence of T in bilayer graphene are plotted in Fig. 2b. They show a dramatic difference as compared with the case of massless Dirac fermions. There are again pronounced transmission resonances at some incident angles, where T approaches unity. However, instead of the perfect transmission found for normally-incident Dirac fermions (see Fig. 2a), our numerical analysis has yielded the opposite effect: Massive chiral fermions are always perfectly reflected for angles close to $\phi = 0$. At the same time, there is always a “magic angle” when the transmission probability is equal to one.

The fact that a barrier (or even a single $p-n$ junction) incorporated in a bilayer graphene device should lead to exponentially small tunneling current can be exploited in developing graphene-based field effect transistors (FET)¹⁶. Such transistors are particularly tempting because of their high mobility and ballistic transport at submicron distances^{7,8,9}. However, the fundamental problem along this route is that the conducting channel in single-layer graphene cannot be pinched off due to the Klein paradox (alternative view on this fact based on the concept of the minimal conductivity will be discussed in the next section). This severely limits achievable on-off ratios for such FETs⁷ and, therefore, the scope for their applications. A bilayer FET with a local gate inverting the sign of charge carriers should yield much higher on-off ratios.

III. PROBLEM OF MINIMUM CONDUCTIVITY

One of amazing properties of graphene is its finite minimal conductivity which is of the order of the conductance quantum e^2/h per valley per spin; it is important to stress that this is the “quantization” of conductivity rather than of conductance⁸. This is not only very interesting conceptually but also important in the view of potential applications of graphene for ballistic field-effect transistors^{7,16}. At the same time, this phenomenon is intimately related with specifically quantum-relativistic phenomenon known as Zitterbewegung^{38,46}.

Numerous considerations of the conductivity of a two-dimensional massless Dirac fermion gas do give this value of the minimal conductivity with accuracy of some factor of the order of unity^{46,47,48,49,50,51,52,53,54,55}. It is really surprising that in this case there is a final conductivity for an *ideal* crystal, that is, without any scattering processes^{46,49,54,55}.

The Dirac Hamiltonian (1) in the secondary-quantization representation takes the form

$$H = v \sum_{\mathbf{p}} \Psi_{\mathbf{p}}^{\dagger} \sigma \mathbf{p} \Psi_{\mathbf{p}} \quad (10)$$

and the corresponding expression for the current operator

$$\mathbf{j} = ev \sum_{\mathbf{p}} \Psi_{\mathbf{p}}^{\dagger} \sigma \Psi_{\mathbf{p}} \quad (11)$$

where \mathbf{p} is the momentum and $\Psi_{\mathbf{p}}^{\dagger} = (\psi_{\mathbf{p}1}^{\dagger}, \psi_{\mathbf{p}2}^{\dagger})$ are pseudospinor electron operators. Here we omit spin and valley indices (so, keeping in mind applications to graphene, the results for the conductivity should be multiplied by 4 due to two spin projections and two valleys). Straightforward calculations result in the following time evolution of the electron annihilation operator

$$\Psi_{\mathbf{p}}(t) = \frac{1}{2} \left[e^{-i\epsilon_{\mathbf{p}}t} \left(1 + \frac{\mathbf{p}\sigma}{p} \right) + e^{i\epsilon_{\mathbf{p}}t} \left(1 - \frac{\mathbf{p}\sigma}{p} \right) \right] \Psi_{\mathbf{p}} \quad (12)$$

and for the current operator

$$\begin{aligned} \mathbf{j}(t) &= \mathbf{j}_0(t) + \mathbf{j}_1(t) + \mathbf{j}_1^{\dagger}(t) \\ \mathbf{j}_0(t) &= ev \sum_{\mathbf{p}} \Psi_{\mathbf{p}}^{\dagger} \frac{\mathbf{p}(\mathbf{p}\sigma)}{p^2} \Psi_{\mathbf{p}} \\ \mathbf{j}_1(t) &= \frac{ev}{2} \sum_{\mathbf{p}} \Psi_{\mathbf{p}}^{\dagger} \left[\sigma - \frac{\mathbf{p}(\mathbf{p}\sigma)}{p^2} + \frac{i}{p} \sigma \times \mathbf{p} \right] \Psi_{\mathbf{p}} e^{2i\epsilon_{\mathbf{p}}t} \end{aligned} \quad (13)$$

where $\epsilon_{\mathbf{p}} = vp/\hbar$ is the particle frequency. The last term in Eq.(13) corresponds to the “Zitterbewegung”, a phenomenon connected with the uncertainty of the position of relativistic quantum particles due to the inevitable creation of particle-antiparticle pairs at the position measurement³⁸.

To calculate the conductivity $\sigma(\omega)$ following Ref.⁴⁶ we will try first to use the Kubo formula⁵⁶ which reads for two-dimensional isotropic case:

$$\sigma(\omega) = \frac{1}{2A} \int_0^{\infty} dt e^{i\omega t} \int_0^{\beta} d\lambda \langle \mathbf{j}(t - i\lambda) \mathbf{j} \rangle \quad (14)$$

where $\beta = T^{-1}$ is the inverse temperature, A is the sample area. In the static limit $\omega = 0$ taking into account the Onsager relations and analyticity of the correlators $\langle \mathbf{j}(z) \mathbf{j} \rangle$ for $-\beta < \text{Im}z \leq 0$ one has⁵⁶

$$\sigma = \frac{\beta}{4A} \int_{-\infty}^{\infty} dt \langle \mathbf{j}(t) \mathbf{j} \rangle. \quad (15)$$

Usually, for ideal crystals, the current operator commutes with the Hamiltonian and thus $\mathbf{j}(t)$ does not depend on time. In that case, due to Eq.(14) the frequency-dependent conductivity contains only the Drude peak

$$\sigma_D(\omega) = \frac{\pi}{2A} \lim_{T \rightarrow 0} \frac{\langle \mathbf{j}^2 \rangle}{T} \delta(\omega) \quad (16)$$

Either the spectral weight of the Drude peak is finite and, thus, the static conductivity is infinite, or it is equal to zero. It is easy to check that for the system under consideration the spectral weight of the Drude peak is proportional to the modulus of the chemical potential $|\mu|$ (cf. Eq.(44) of Ref.⁵³) and thus vanishes at zero doping ($\mu = 0$). It is the Zitterbewegung, i.e. the oscillating term $\mathbf{j}_1(t)$ which is responsible for nontrivial behavior of the conductivity for zero temperature and zero chemical potential (that is, the case of no charge carriers). A straightforward calculation gives a formal result

$$\sigma = \frac{\pi e^2}{2h} \int_0^\infty d\epsilon \epsilon \delta^2(\epsilon) \quad (17)$$

where one delta-function originates from the integration over t in Eq.(15) and the second one - from the derivative of the Fermi distribution function appearing at the calculation of the average over product of Fermi-operators. Of course, the square of the delta function is not a well-defined object and thus Eq.(17) is meaningless before specification of the way how one should regularize the delta-functions. After regularization the integral in Eq.(17) is finite, but its value depends on the regularization procedure (see Refs.^{49,55}).

To circumvent the problem of ambiguity in the expression for σ in Eq.(17) it is instructive to follow the alternative Landauer approach to calculate the conductivity^{57,58}. Let us assume that our sample is the ring of length L_y in y direction; we will use the Landauer formula to calculate the conductance in the x direction (see Fig. 3). There is still an uncertainty in the sense that the conductivity turns out to be dependent on the shape of the sample. To have a final transparency we should keep L_x finite. On the other hand, periodic boundary conditions in y direction are nonphysical and we have to choose L_y as large as possible to weaken their effects. Thus, for two-dimensional situation one should choose $L_x \ll L_y$.

In the coordinate representation the Dirac equation at zero energy takes the form

$$\begin{aligned} (K_x + iK_y)\psi_1 &= 0 \\ (K_x - iK_y)\psi_2 &= 0 \end{aligned} \quad (18)$$

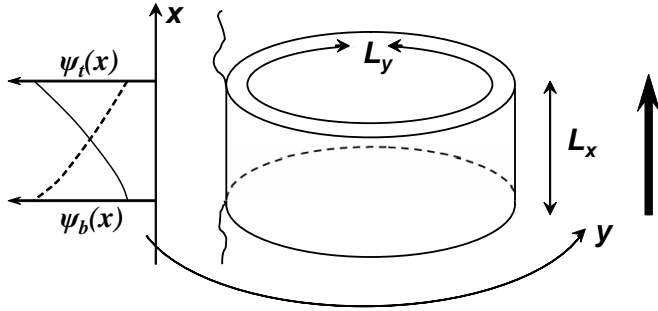


FIG. 3: Geometry of the sample. The thick arrow shows the direction of current. ψ_t (solid line) and ψ_b (dashed line) are wave functions of the edge states localized near the top and the bottom of the sample, correspondingly.

where $K_i = -i\frac{\partial}{\partial x_i}$. General solutions of these equations are just arbitrary analytical (or complex conjugated analytical) functions:

$$\begin{aligned} \psi_1 &= \psi_1(x + iy), \\ \psi_2 &= \psi_2(x - iy). \end{aligned} \quad (19)$$

Due to periodicity in the y direction both wave functions should be proportional to $\exp(ik_y y)$ where $k_y = 2\pi n/L_y, n = 0, \pm 1, \pm 2, \dots$. This means that the dependence on x is also fixed: the wave functions are proportional to $\exp(\pm 2\pi n x/L_y)$. They correspond to the states localized near the bottom and the top of the sample (see Fig. 3).

To use the Landauer formula, we should introduce boundary conditions at the sample edges ($x = 0$ and $x = L_x$). To be specific, let us assume that the leads are made of doped graphene with the potential $V_0 < 0$ and the Fermi energy $E_F = v k_F = -V_0$. The wave functions in the leads are supposed to have the same y -dependence, that is, $\psi_{1,2}(x, y) = \psi_{1,2}(x) \exp(ik_y y)$. Thus, one can try the solution of the Dirac equation in the following form:

$$\psi_1(x) = \begin{cases} e^{ik_x x} + r e^{-ik_x x}, & x < 0 \\ a e^{k_y x}, & 0 < x < L_x \\ t e^{ik_x x}, & x > L_x \end{cases}$$

$$\psi_2(x) = \begin{cases} e^{ik_x x + i\phi} - r e^{-ik_x x - i\phi}, & x < 0 \\ b e^{-k_y x}, & 0 < x < L_x \\ t e^{ik_x x + i\phi}, & x > L_x \end{cases} \quad (20)$$

where $\sin \phi = k_y/k_F$, $k_x = \sqrt{k_F^2 - k_y^2}$. From the conditions of the continuity of the wave functions, one can find the transmission coefficient

$$T_n = |t(k_y)|^2 = \frac{\cos^2 \phi}{\cosh^2(k_y L_x) - \sin^2 \phi}. \quad (21)$$

Furthermore, one should assume that $k_F L_x \gg 1$ and put $\phi \simeq 0$ in Eq.(21). Thus, the trace of the transparency which is just the conductance (in units of e^2/h) is

$$TrT = \sum_{n=-\infty}^{\infty} \frac{1}{\cosh^2(k_y L_x)} \simeq \frac{L_y}{\pi L_x}. \quad (22)$$

Assuming that the conductance is equal to $\sigma \frac{L_y}{L_x}$ one finds the contribution to the conductivity equal to $e^2/(\pi h)$. Experimentally⁸, it is close to e^2/h , that is, roughly, three times larger than this estimation. This discrepancy known as a “missed pi(e) problem” is still not solved.

One should stress that this is the gapless character of the spectrum and the chirality rather than the linear dispersion relation which lead to the minimal conductivity. Different estimations for the bilayer graphene give the same order of magnitude for the conductivity^{46,59,60,61,62,63}, in agreement with experimental observations³⁵.

Another approach to qualitative understanding of the minimal conductivity is based on the Klein paradox¹⁶. In conventional 2D systems, strong enough disorder results in electronic states that are separated by barriers with exponentially small transparency^{64,65}. This is known to lead to the Anderson localization. In contrast, in both graphene materials all potential barriers are relatively transparent ($T \approx 1$ at least for some angles) which does not allow charge carriers to be confined by potential barriers that are smooth on an atomic scale. Therefore, different electron and hole “puddles” induced by disorder are not isolated but effectively percolate, thereby suppressing localization. In the absence of the localization, a standard Mott estimation of the minimal conductivity assuming that the mean-free path cannot be smaller than electron wave-length⁶⁶ immediately gives the minimal conductivity $\approx e^2/h$ ⁶⁷.

IV. INDEX THEOREM AND ANOMALOUS QUANTUM HALL EFFECT

The anomalous QHE in graphene^{8,9} is probably the most striking demonstration of the massless character of the charge carrier spectrum in graphene. In two-dimensional systems with a constant magnetic field \mathbf{B} perpendicular to the system plane the energy spectrum is discrete (Landau quantization). For the case of massless Dirac fermions the energy spectrum takes the form^{68,69}

$$E_{\nu\sigma} = \sqrt{2|e|B\hbar v_F^2(\nu + 1/2 \pm 1/2)} \quad (23)$$

where v_F is the electron velocity, $\nu = 0, 1, 2, \dots$ is the quantum number and the term with $\pm 1/2$ is connected to the chirality. Just to remind that in the usual case of the parabolic dispersion relation the Landau level sequence is $E = \hbar\omega_c(\nu + 1/2)$ where ω_c is the frequency of electron rotation in magnetic field (cyclotron frequency)^{20,70}.

An important peculiarity of Landau levels for massless Dirac fermions is the existence of zero-energy states (with $\nu = 0$ and the minus sign in equation (23)). This situation differs fundamentally from usual semiconductors with parabolic bands where the first Landau level is shifted by $\hbar\omega_c/2$. The existence of the zero-energy Landau level leads to an anomalous QHE with *half-integer* quantization of the Hall conductivity, instead of the *integer* one (for a review of the QHE, see, e.g., Ref.⁷¹). Usually, all Landau levels have the same degeneracy (a number of electron states with a given energy) which is just proportional to a magnetic flux through the system. As a result, plateaus in the Hall conductivity corresponding to the filling of the first ν levels are just integer (in units of the conductance quant e^2/h). For the case of massless Dirac electrons, the zero-energy Landau level has twice smaller degeneracy than any other level (it corresponds to the minus sign in the equation (1) whereas the energy level proportional to \sqrt{p} with integer $p \geq 1$ are obtained twice, for $\nu = p$ and minus sign, and for $\nu = p - 1$ and plus sign). A discovery of this “half-integer QHE”^{8,9} was the most direct evidence of the Dirac fermions in graphene.

A deeper view on the origin of the zero-energy Landau level and thus the anomalous QHE is provided by the famous Atiyah-Singer index theorem which plays an important role in the modern quantum field theory and theory of superstrings⁷². The Dirac equation has a charge-conjugation symmetry between electrons and holes. This means that for any electron state with a positive energy E a corresponding conjugated hole state with the energy $-E$ should exist. However, the states with zero energy can be, in general, anomalous. For

curved space (e.g., for a deformed graphene sheet with some defects of crystal structure) and/or in the presence of so called “gauge fields” (the usual electromagnetic field provides just the simplest example of these fields) sometimes an existence of states with zero energy is guaranteed by topological reasons, this states being chiral (in our case this means that depending on the sign of the magnetic field there is only sublattice A or sublattice B states which contribute to the zero-energy Landau level). This means, in particular, that the number of these states expressed in terms of total magnetic flux is a topological invariant and remains the same even if the magnetic field is inhomogeneous⁸. This is an important conclusion since, as discussed in section 1, the ripples on graphene create strong effective inhomogeneous magnetic fields leading, in particular, to suppression of weak localization²³. However, due to these topological arguments they cannot destroy the anomalous QHE in graphene. About applications of the index theorem to two-dimensional systems, and, in particular, to graphene see also Refs.^{73,74}.

An alternative view on the origin of the anomalous QHE in graphene is based on the concept of the “Berry phase” which was discussed above in connection with the Klein paradox. When chiral electron moves along the close contour its wave function gains an additional phase $\phi = \pi$. In quasiclassical terms (see, e.g., Refs.^{20,75}), stationary states are nothing but electron standing waves and they can exist if the electron orbit contains, at least, half of the wavelength. Due to the additional phase shift by the Berry phase, this condition is satisfied already for the zeroth length of the orbit, that is, for zero energy. Other aspects of the QHE in graphene are considered in papers^{76,77,78,79}.

In the previous section we have discussed an absence of localization in graphene as one of the main consequences of relativistic quantum effects such as the Klein paradox. At the same time, the localization is of crucial importance for the QHE providing a well-defined Hall plateau⁷¹. Here we demonstrate that the localization by a scalar potential V in the magnetic field is possible. For simplicity, let us assume the case of a weak one-dimensional inhomogeneity with the potential $V = V(y)$ much smaller than the cyclotron quantum of the order of $\hbar v_F/l$ where $l = (\hbar c/|e|B)^{1/2}$ is the magnetic length.

Using a standard gauge for the vector potential $A_x = A_z = 0, A_y = Bx$ one can write the Dirac Hamiltonian for the problem as

$$\hat{H} = \hat{H}_1 + \hat{H}_2 \quad (24)$$

where

$$\hat{H}_1 = \begin{pmatrix} 0 & -i\hbar v_F \left(\frac{\partial}{\partial x} - \frac{x}{l^2} \right) \\ -i\hbar v_F \left(\frac{\partial}{\partial x} + \frac{x}{l^2} \right) & 0 \end{pmatrix}, \quad (25)$$

$$\hat{H}_2 = \begin{pmatrix} V(y) & \hbar v_F \frac{\partial}{\partial y} \\ -\hbar v_F \frac{\partial}{\partial y} & V(y) \end{pmatrix}. \quad (26)$$

Let us try eigenfunctions of the Hamiltonian (24) with the energy E as an expansion in the basis of appropriate harmonic oscillator problem:

$$\begin{aligned} \psi_i &= \sum_{\nu=0}^{\infty} \int \frac{dk_y}{2\pi} c_{\nu}^{(i)}(k_y) e^{ik_y y} \varphi_{\nu}(k_y, x), \\ \varphi_{\nu}(k_y, x) &= D_{\nu} \left(\frac{\sqrt{2}(x - l^2 k_y)}{l} \right), \end{aligned} \quad (27)$$

where $i = 1, 2$ is the pseudospinor index and $D_{\nu}(z) \sim \exp(-z^2/4) H_{\nu}(z/\sqrt{2})$ the Weber functions⁸⁰. After straightforward calculations one obtains a set of equations for the expansion coefficients $c_{\nu}^{(i)}(k_y)$:

$$\begin{aligned} -\frac{\sqrt{2}}{l} (1 - \delta_{\nu,0}) c_{\nu}^{(2)}(k_y) &= \frac{iE}{\hbar v_F} c_{\nu}^{(1)}(k_y) - \frac{i}{\hbar v_F} \sum_{\nu'=0}^{\infty} \int \frac{dq_y}{2\pi} v(k_y - q_y) c_{\nu'}^{(1)}(q_y) \langle \nu, k_y | \nu', q_y \rangle, \\ \frac{\sqrt{2}}{l} (1 + \nu) c_{\nu}^{(1)}(k_y) &= \frac{iE}{\hbar v_F} c_{\nu}^{(2)}(k_y) - \frac{i}{\hbar v_F} \sum_{\nu'=0}^{\infty} \int \frac{dq_y}{2\pi} v(k_y - q_y) c_{\nu'}^{(2)}(q_y) \langle \nu, k_y | \nu', q_y \rangle, \\ \langle \nu, k_y | \nu', q_y \rangle &= \int dx \varphi_{\nu}(k_y, x) \varphi_{\nu'}(q_y, x), \end{aligned} \quad (28)$$

$v(q)$ is a Fourier component of $V(y)$. For the case of a weak ($|V(y)| \ll \hbar v_F/l$) and smooth potential one can neglect a mixing of different Landau bands, similar to the case of QHE for conventional electron gas⁷¹. As a result of direct calculations one can demonstrate that in this case the solution of Eq.(28) describes the Landau wave functions of nonperturbed problem with the orbit center y_0 satisfying the equation

$$E \pm \frac{\hbar v_F}{l} \sqrt{2\nu} = V(y_0). \quad (29)$$

Thus, the Landau levels in the case under consideration are just smeared into the bands of localized states with the localization radius of order of the magnetic length, similar to the case of the usual QHE⁷¹.

V. NONLINEAR SCREENING OF CHARGE IMPURITIES

In QED, vacuum polarization effects due to creation of virtual electron-positron pairs by an external potential are of a crucial importance^{81,82}. Due to the smallness of the fine structure constant $\alpha_{QED} = e^2/\hbar c \simeq 1/137$ these effects leading to logarithmic corrections to the Coulomb potential are rather small, except the case of very small distances. In graphene, the effective fine structure constant $\alpha = e^2/\hbar v_F \epsilon$ is of the order of unity (ϵ is the dielectric constant due to substrate; for the case of graphene on quartz one should choose⁸³ $\epsilon \simeq 2.4 - 2.5$) and the corresponding effects can be of crucial importance for transport properties⁸⁴. Due to the absence of explicitly small parameters describing correlation effects in graphene it is very difficult to consider this problem rigorously and the situation still is controversial. Nevertheless, the vacuum polarization effects are in our opinion important and should be taken into account in any future theory.

A general nonlinear theory of screening in the system of interacting particles can be formulated in a framework of the density functional approach⁸⁵. In this theory a total potential $V(\mathbf{r})$ acting on electrons is equal

$$V(\mathbf{r}) = V_0(\mathbf{r}) + V_{ind}(\mathbf{r}) \quad (30)$$

where $V_0(\mathbf{r})$ is an external potential and $V_{ind}(\mathbf{r})$ is a potential induced by a redistribution of electron density:

$$V_{ind}(\mathbf{r}) = \frac{e^2}{\epsilon} \int d\mathbf{r}' \frac{n(\mathbf{r}') - \bar{n}}{|\mathbf{r} - \mathbf{r}'|} + V_{xc}(\mathbf{r}), \quad (31)$$

where the first term is the Hartree potential and the second one is the exchange-correlation potential. We consider here only a redistribution of charge carriers in the external impurity potential

$$V_0(\mathbf{r}) = \frac{Ze^2}{\epsilon r}. \quad (32)$$

taking into account contributions of the crystal lattice potential and of electrons in completely filled bands via a dielectric constant ϵ and compensated homogeneous charge density $-e\bar{n}$. Here Z is the dimensionless impurity charge (to be specific, we will assume $Z > 0$; it can be easily demonstrated that, actually, in our final expressions Z should be just replaced by $|Z|$). This kind of approach is valid at a spacial scale much larger than a lattice constant; in all other aspects, it is formally exact until we specify the expressions for V_{xc} and $n[V(\mathbf{r})]$.

The Thomas-Fermi theory⁸⁶ which is, actually, the simplest approximation in the density functional approach, was used in Ref.⁸⁴. It is based on the two assumptions: (i) we neglect the exchange-correlation potential in comparison with the Hartree potential in Eq.(31) and (ii) we put $n(\mathbf{r}') = n[\mu - V(\mathbf{r}')]$, where $n(\mu)$ is a density of a homogeneous electron gas with chemical potential μ . The former assumption means that we are interested in the long-wavelength response of the electron system and thus the long-range Coulomb forces dominate over the local exchange-correlation effects. The latter one holds provided that the external potential is smooth enough. A rigorous statement is that an addition of a *constant* potential is equivalent to the shift of the chemical potential. In particular, the Thomas-Fermi theory gives an exact expression for a static inhomogeneous dielectric function $\epsilon(q)$ in the limit of small wavevectors $q \rightarrow 0$ ²⁰. The Thomas-Fermi theory of atoms is asymptotically exact in the limit of infinite nuclear charge⁸⁶.

In the Thomas-Fermi theory Eq.(31) reads

$$V_{ind}(\mathbf{r}) = \frac{e^2}{\epsilon} \int d\mathbf{r}' \frac{n[\mu - V(\mathbf{r}')] - n(\mu)}{|\mathbf{r} - \mathbf{r}'|}. \quad (33)$$

The function $n(\mu)$ is expressed via the density of states $N(E)$:

$$n(\mu) = \int dE f(E) N(E) = \int^{\mu} dE N(E) \quad (34)$$

where $f(E)$ is the Fermi function, and the last equality is valid for zero temperature (we will restrict ourselves here only to this case). For the case of graphene with the linear energy spectrum near the crossing points K and K' one has

$$n(\mu) = \frac{1}{\pi} \frac{\mu |\mu|}{\hbar^2 v_F^2}, \quad (35)$$

where we have taken into account a factor 4 due to two valleys and two spin projections.

Let us start first with the case of zero doping ($\mu = 0$) where, according to the linear response theory, there is no screening at all. Substituting Eqs.(33), (32), and (35) into Eq.(30), introducing the notation

$$V(r) = \frac{e^2}{\epsilon r} F(r) \quad (36)$$

and integrating over the polar angle of vector \mathbf{r}' , we obtain a nonlinear integral equation for the function $F(r)$:

$$F(r) = Z - \frac{2Q}{\pi} \int_0^\infty \frac{dr'}{r'} \frac{r}{r+r'} K\left(\frac{2\sqrt{rr'}}{r+r'}\right) F^2(r') \quad (37)$$

where

$$K(k) = \int_0^{\pi/2} \frac{d\varphi}{\sqrt{1 - k^2 \sin^2 \varphi}} \quad (38)$$

is the complete elliptic integral,

$$Q = 2 \left(\frac{e^2}{\epsilon \hbar v_F} \right)^2; \quad (39)$$

for the case of graphene on SiO_2 $Q \simeq 2$.

An approximate solution of the integral equation (37) at $r \gg a$ gives the following result⁸⁴

$$F(r) \simeq \frac{Z}{1 + ZQ \ln \frac{r}{a}} \quad (40)$$

which is formally similar to that in QED⁸² but with a much larger value of the interaction constant. Note that logarithmically divergent corrections to the electron effective mass in undoped graphene due to the vacuum polarization effects have been considered in Ref.⁸⁷.

For the case of doped graphene the main result of Ref.⁸⁴ is the replacement of the bare charge impurity Z by

$$Z^* \simeq \frac{Z}{1 + ZQ \ln \frac{1}{\kappa a}}. \quad (41)$$

where

$$\kappa = \frac{4e^2 |\mu|}{\epsilon \hbar^2 v_F^2} \quad (42)$$

is the inverse screening radius. This weakens essentially this scattering mechanism since $Q \ln \frac{1}{\kappa a}$ is of order of ten for typical charge carrier concentrations. Perturbative estimations of the electron mobility⁸⁸ should be thus multiplied by this factor squared. As a result, the mobility for the same parameters turns out to be two order of magnitude larger. Instead of a concentration-independent mobility, we obtain a mobility proportional to $\ln^2(k_F a)$. More accurately, one should use an expression for the mobility obtained by Ando⁸³ (see Eq.(3.27) and Fig. 5 of that paper) but with the replacement of Z by Z^* when calculating the strength of the Coulomb interaction.

VI. SCATTERING OF DIRAC FERMIONS BY SHORT-RANGE IMPURITY POTENTIAL

Here we will discuss quantum relativistic effects in the electrons scattering by a short-range potential. It appears that in the case of graphene the contribution of such defects to

the resistivity is essentially smaller than for the conventional nonrelativistic two-dimensional electron gas. We argue that this conclusion should help our understanding of remarkably high charge carrier mobilities observed in graphene^{7,8,9}.

Let us consider the case of a small concentration of point defects (to be specific, we will call them impurities) with the concentration n_{imp} and the angle-dependent scattering cross-section $\sigma(\phi)$. Then the defect contribution to the resistivity ρ reads⁵¹

$$\begin{aligned} \rho &= \frac{2}{e^2 v_F^2 N(E_F)} \frac{1}{\tau(k_F)}, \\ \frac{1}{\tau(k_F)} &= n_{imp} v_F \int_0^{2\pi} d\phi \frac{d\sigma(\phi)}{d\phi} (1 - \cos \phi) \end{aligned} \quad (43)$$

where $N(E_F) = 2k_F/\pi\hbar v_F$ is the density of states at the Fermi level (taking into account the double spin degeneracy and two valleys), τ is the mean-free path. Note that the product $v_F N(E_F)$ is proportional to $k_F = \sqrt{\pi n}$ (n is the electron concentration) for both ultrarelativistic and nonrelativistic two-dimensional electron gas and thus any essential difference in their transport properties can be related only to the scattering cross-section.

To determine the scattering cross section one has to solve the two-dimensional Dirac equation which, for the case of massless particles and radially symmetric scattering potential $V(r)$ takes the form (cf. Ref.³⁸ for three-dimensional case):

$$\begin{aligned} \frac{dg_l(r)}{dr} - \frac{l}{r} g_l(r) - \frac{i}{\hbar v_F} [E - V(r)] f_l(r) &= 0, \\ \frac{df_l(r)}{dr} + \frac{l+1}{r} f_l(r) - \frac{i}{\hbar v_F} [E - V(r)] g_l(r) &= 0, \end{aligned} \quad (44)$$

where $l = 0, \pm 1, \dots$ is the angular-momentum quantum number, $g_l(r) e^{il\phi}$ and $f_l(r) e^{i(l+1)\phi}$ are components of the Dirac pseudospinor; to be specific we will consider the case of electrons $E = \hbar v_F k > 0$.

Modifying a standard scattering theory⁸⁹ for the two-dimensional case one should try the solutions of Eq.(44) outside the region of action of the potential in the form

$$\begin{aligned} g_l(r) &= A \left[J_l(kr) + t_l H_l^{(1)}(kr) \right], \\ f_l(r) &= iA \left[J_{l+1}(kr) + t_l H_{l+1}^{(1)}(kr) \right], \end{aligned} \quad (45)$$

where the terms proportional to Bessel (Hankel) functions describe incident (scattering)

waves,

$$\frac{d\sigma(\phi)}{d\phi} = \frac{2}{\pi k} \left| \sum_{l=-\infty}^{\infty} t_l e^{il\phi} \right|^2. \quad (46)$$

The Dirac equation for ultrarelativistic particles (44) has an important symmetry with respect to replacement $f \longleftrightarrow g, l \longleftrightarrow -l - 1$ which means $t_l = t_{-l-1}$. Thus, Eq.(46) can be rewritten in the form

$$\frac{d\sigma(\phi)}{d\phi} = \frac{2}{\pi k} \left| \sum_{l=0}^{\infty} t_l \cos[(l + 1/2)\phi] \right|^2. \quad (47)$$

The back scattering ($\phi = \pi$) is absent rigorously, as was discussed in the section 2.

For the simplest case of the potential $V(r) = V_0$ at $r < R$ and $V(r) = 0$ at $r > R$, using boundary conditions of continuity of the wave functions at $r = R$ one finds

$$t_l(k) = \frac{J_l(qR) J_{l+1}(kR) - J_l(kR) J_{l+1}(qR)}{H_l^{(1)}(kR) J_{l+1}(qR) - J_l(qR) H_{l+1}^{(1)}(kR)} \quad (48)$$

where $q = (E - V_0)/\hbar v_F$. For the case of small energy, $E \ll V_0, kR \ll 1$ which is typical for graphene one has

$$t_l(k) \simeq \frac{\pi i}{(l!)^2} \frac{J_{l+1}(qR)}{J_l(qR)} \left(\frac{kR}{2} \right)^l \quad (49)$$

and thus the s -scattering ($l = 0$) dominates. Substituting Eq.(49) into Eqs.(47) and (43), one finds the estimation for the impurity contribution to the resistivity $\rho \simeq (h/4e^2) n_{imp} R^2$. This means that scattering centers with the radius of potential R of order of interatomic distances and small concentration are irrelevant for the electron transport in graphene giving negligible contribution to the resistivity.

If we would repeat the same calculations for nonrelativistic electron gas⁹⁰ we would obtain, instead of Eq.(48)

$$t_l(k) = \frac{(k/q) J_l(qR) J_{l+1}(kR) - J_l(kR) J_{l+1}(qR)}{H_l^{(1)}(kR) J_{l+1}(qR) - (k/q) J_l(qR) H_{l+1}^{(1)}(kR)} \quad (50)$$

where k and q are, again, wavevectors outside and inside the potential region. In this case the s -scattering phase vanishes for small energies not linearly but only logarithmically and one obtains much larger resistivity

$$\rho \simeq \frac{h}{4e^2} \frac{n_{imp}}{n} \ln^2(k_F R) \quad (51)$$

(note that the same estimation holds for the case of massless Dirac electrons in a particular case of the resonant scattering when $J_0(qR) = 0$).

So, the basic conclusion is that whenever any potential works as a resonant scatterer in the case of massive particles, the scattering is non-resonant in the case of massless Dirac fermions in graphene, except some special values of parameters.

Conclusions

The examples considered demonstrate that graphene provides an unexpected bridge between the condensed matter physics and quantum field theory. The impact of the experimental discovery of this material on different areas of physics and industry can't be overestimated. First of all, graphene is the first example of truly two-dimensional crystals, in contrast with numerous *quasi*-two-dimensional crystals known before. This opens many interesting questions concerning thermodynamics, lattice dynamics and structural properties of such systems which are, however, beyond the scope of this paper. Furthermore, single-layer graphene provides first experimental realization of a two-dimensional massless Dirac fermion system. The analogy with the quantum field theory proved crucial for understanding of graphene unusual electronic properties, such as anomalous QHE, absence of the Anderson localization, inefficiency of scattering by point defects, etc. The bilayer graphene has a very unusual gapless parabolic spectrum providing an example of the system with electron wave equation different from both Dirac and Schrödinger ones.

Acknowledgements. We are thankful to Andre Geim, Maria Vozmediano, and Leonid Levitov for helpful discussions. This work was supported by the Stichting voor Fundamenteel Onderzoek der Materie (FOM), the Netherlands and by the Royal Society, UK.

¹ R.F. Curl, Rev. Mod. Phys. 69 (1997) 691.

² H. Kroto, Rev. Mod. Phys. 69 (1997) 703.

³ R.E. Smalley, Rev. Mod. Phys. 69 (1997) 723.

⁴ S. Iijima, Nature 354 (1991) 56.

⁵ P.R. Wallace, Phys. Rev. 71 (1947) 622.

⁶ K.S. Novoselov, D. Jiang, F. Schedin, T.J. Booth, V.V. Khotkevich, S.M. Morozov, and A.K. Geim, PNAS 102 (2005) 10451.

⁷ K.S. Novoselov, A.K. Geim, S.V. Morozov, D. Jiang, Y. Zhang, S.V. Dubonos, I.V. Grigorieva, and A.A. Firsov, *Science* 306 (2004) 666.

⁸ K.S. Novoselov, A.K. Geim, S.V. Morozov, D. Jiang, M.I. Katsnelson, I.V. Grigorieva, S.V. Dubonos, and A.A. Firsov, *Nature* 438 (2005) 197.

⁹ Y. Zhang, Y.-W. Tan, H.L. Stormer, and P. Kim, *Nature* 438 (2005) 201.

¹⁰ A.K. Geim and K.S. Novoselov, *Nature Mater.* 6 (2007) 183.

¹¹ M.I. Katsnelson, *Mater. Today* 10, Issue 1&2 (2007) 20.

¹² D.H. Perkins, *Introduction to High Energy Physics*, Cambridge Unive. Press, Cambridge, 2000.

¹³ R.V. Pound and G.A. Rebka, *Phys. Rev. Lett.* 4 (1960) 337.

¹⁴ O. Klein, *Z. Phys.* 53 (1929) 157.

¹⁵ N. Dombey and A. Calogeracos, *Phys. Rep.* 315 (1999) 41.

¹⁶ M.I. Katsnelson, K.S. Novoselov, and A.K. Geim, *Nature Phys.* 2 (2006) 620.

¹⁷ J.C. Slonczewski and P.R. Weiss, *Phys. Rev.* 109 (1958) 272.

¹⁸ G.W. Semenoff, *Phys. Rev. Lett.* 53 (1984) 2449.

¹⁹ F.D.M. Haldane, *Phys. Rev. Lett.* 61 (1988) 2015.

²⁰ S.V. Vonsovsky and M.I. Katsnelson, *Quantum Solid State Physics*, Springer, N.Y., 1989.

²¹ D. Boyanovsky, R. Blankenbecler, and R. Yahalom, *Nucl. Phys. B* 270 (1986) 483.

²² A. Shapere and F. Wilczek (Editors), *Geometrical Phases in Physics*, World Scientific, Singapore, 1989.

²³ S.V. Morozov, K.S. Novoselov, M.I. Katsnelson, F. Schedin, L.A. Ponomarenko, D. Jiang, and A.K. Geim, *Phys. Rev. Lett.* 97 (2006) 016801.

²⁴ J.C. Meyer, A.K. Geim, M.I. Katsnelson, K.S. Novoselov, T.J. Booth, and S. Roth, *Nature* 445 (2007).

²⁵ R.E. Peierls, *Helv. Phys. Acta* 7 (1934) 81.

²⁶ R.E. Peierls, *Ann. Inst. H. Poincare* 5 (1935) 177.

²⁷ L.D. Landau, *Phys. Z. Sowjet Union* 11 (1937) 26.

²⁸ L.D. Landau and E.M. Lifshitz, *Statistical Physics, Part I*, Pergamon Press, Oxford, 1980.

²⁹ D.R. Nelson, T. Piran, and S. Weinberg (Editors), *Statistical Mechanics of Membranes and Surfaces*, World Scientific, Singapore, 2004).

³⁰ D.R. Nelson and L. Peliti, *J. Physique* 48 (1987) 1085.

³¹ L. Radzhovsky and P. Le Doussal, *Phys. Rev. Lett.* 69 (1992) 1209.

³² S.V. Iordanskii and A.E. Koshelev, JETP Lett. 41 (1985) 574.

³³ P.E. Lammert and V.H. Crespi, Phys. Rev. B 61 (2000) 7308.

³⁴ A. Cortijo and M.A.H. Vozmediano, cond-mat/0603717.

³⁵ K.S. Novoselov, E. McCann, S.V. Morozov, V.I. Falko, M.I. Katsnelson, U. Zeitler, D. Jiang, F. Schedin, and A.K. Geim, Nature Phys. 2 (2006) 177.

³⁶ E. McCann and V.I. Falko, Phys. Rev. Lett. 96 (2006) 086805.

³⁷ B. Partoens and F.M. Peeters, Phys. Rev. B 74 (2006) 075404.

³⁸ V. B. Berestetskii, E. M. Lifshitz, and L. P. Pitaevskii, Relativistic Quantum Theory, vol. 1, Pergamon, Oxford, 1971.

³⁹ W. Greiner, B. Mueller, and J. Rafelski, Quantum Electrodynamics of Strong Fields, Springer, Berlin, 1985.

⁴⁰ A.A. Grib, S.G. Mamayev, and V.M. Mostepanenko, Vacuum Effects in Strong Fields, Friedmann, St.-Petersburg, 1994.

⁴¹ D.N. Page, New J. Phys. 7 (2005) 203.

⁴² V.V. Cheianov and V.I. Falko, Phys. Rev. B 74 (2006) 041403(R).

⁴³ J.M. Pereira, V. Mlinar, F.M. Peeters, and P. Vasilopoulos, Phys. Rev. B 74 (2006) 045424.

⁴⁴ T. Ando, T. Nakanishi, and R. Saito, J. Phys. Soc. Japan 67 (1998) 2857.

⁴⁵ P.L. McEuen, M. Bockrath, D.H. Cobden, Y.G. Yoon, and S.G. Louie, Phys. Rev. Lett. 83 (1999) 5098.

⁴⁶ M.I. Katsnelson, Eur. Phys. J. B 51 (2006) 157.

⁴⁷ E. Fradkin, Phys. Rev. B 33 (1986) 3263.

⁴⁸ P. A. Lee, Phys. Rev. Lett. 71 (1993) 1887.

⁴⁹ A.W.W. Ludwig, M.P.A. Fisher, R. Shankar, and G. Grinstein, Phys. Rev. B 50 (1994) 7526.

⁵⁰ A. A. Nersesyan, A. M. Tsvelik, and F. Wenger, Phys. Rev. Lett. 72 (1994) 2628.

⁵¹ N. H. Shon and T. Ando, J. Phys. Soc. Japan 67 (1998) 2421.

⁵² E. V. Gorbar, V. P. Gusynin, V. A. Miransky, and I. A. Shovkovy, Phys. Rev. B 66 (2002) 045108.

⁵³ X. Yang and C. Nayak, Phys. Rev. B 65 (2002) 064523.

⁵⁴ J. Tworzydlo, B. Trauzettel, M. Titov, A. Rycerz, and C.W.J. Beenakker, Phys. Rev. Lett. 96 (2006) 246802.

⁵⁵ K. Ziegler, Phys. Rev. Lett. 97 (2006) 266802.

⁵⁶ D.N. Zubarev, *Nonequilibrium Statistical Thermodynamics*, Consultants Bureau, New York, 1974.

⁵⁷ C.W.J. Beenakker and H. van Houten, *Solid State Phys.* **44** (1991) 1.

⁵⁸ Ya.M. Blanter and M. Büttiker, *Phys. Rep.* **336** (2000) 1.

⁵⁹ M. I. Katsnelson, *Eur. Phys. J. B* **52** (2006) 151.

⁶⁰ M. Koshino and T. Ando, *Phys. Rev. B* **73** (2006) 245403.

⁶¹ J. Nilsson, A.H. Castro Neto, F. Guinea, and N.M.R. Peres, *Phys. Rev. Lett.* **97** (2006) 266801.

⁶² J. Cserti, *Phys. Rev. B* **75** (2007) 033405.

⁶³ I. Snyman and C.W.J. Beenakker, *Phys. Rev. B* **75** (2007) 045322.

⁶⁴ J.M. Ziman, *Models of Disorder*, Cambridge Univ. Press, Cambridge, 1979.

⁶⁵ I.M. Lifshitz, S.A. Gredeskul, and L.A. Pastur, *Introduction to the Theory of Disordered Systems*, Wiley, New York, 1988.

⁶⁶ N.F. Mott, *Metal-Insulator Transitions*, Taylor and Francis, London, 1974.

⁶⁷ The Mott argument to explain the observed minimal metallic conductivity of graphene was first invoked by A. Geim (private communication).

⁶⁸ J.W. McClure, *Phys. Rev.* **104** (1956) 666.

⁶⁹ V.P. Gusynin and S.G. Sharapov, *Phys. Rev. B* **71** (2005) 125124.

⁷⁰ N.W. Ashcroft and N.D. Mermin, *Solid State Physics*, Holt, Rinehart and Winston, N.Y., 1976.

⁷¹ R.E. Prange and S.M. Girvin (Editors), *The Quantum Hall Effect*, Springer, N.Y., 1987.

⁷² M. Kaku, *Introduction to Superstrings*, Springer, N.Y., 1988.

⁷³ T. Tenjinbayashi, H. Igarashi, and T. Fujiwara, *Ann. Phys. (N.Y.)* **322** (2007) 460.

⁷⁴ J.K. Pach and M. Stone, *cond-mat/0607394*.

⁷⁵ G.P. Mikitik and Yu.V. Sharlai, *Phys. Rev. Lett.* **82** (1999) 2147.

⁷⁶ D.A. Abanin, P.A. Lee, and L.S. Levitov, *Phys. Rev. Lett.* (2006) **96**, 176803.

⁷⁷ V.P. Gusynin and S.G. Sharapov, *Phys. Rev. Lett.* **95** (2005) 146801.

⁷⁸ N.M.R. Peres, F. Guinea, and A.H. Castro Neto, *Phys. Rev. B* **73** (2006) 125411.

⁷⁹ A.H. Castro Neto, F. Guinea, and N.M.R. Peres, *Phys. Rev. B* **73** (2006) 205408.

⁸⁰ E.T. Whittaker and G.N. Watson, *A Course of Modern Calculus*, Cambridge Univ. Press, Cambridge, 1996.

⁸¹ E.M. Lifshitz and L.P. Pitaevskii, *Relativistic Quantum Theory, Part 2*, Pergamon, Oxford, 1977.

⁸² A.B. Migdal, Qualitative Methods in Quantum Theory, Benjamin, Reading, Mass., 1977.

⁸³ T. Ando, J. Phys. Soc. Japan 75 (2006) 074716.

⁸⁴ M.I. Katsnelson, Phys. Rev. B 74 (2006) 201401(R).

⁸⁵ P. Hohenberg and W. Kohn, Phys. Rev. 136 (1964) B884.

⁸⁶ E.H. Lieb, Rev. Mod. Phys. 53 (1981) 603.

⁸⁷ J. Gonzales, F. Guinea, and M.A.H. Vozmediano, Nucl. Phys. B 424 (1994) 595.

⁸⁸ K. Nomura and A.H. MacDonald, Phys. Rev. Lett. 96 (2006) 256602.

⁸⁹ R.G. Newton, Scattering Theory of Waves and Particles, McGraw Hill, N.Y., 1966.

⁹⁰ S.K. Adhikari, Amer. J. Phys. 54 (1986) 362.